Progress In Electromagnetics Research, Vol. 129, 251–269, 2012

MULTIOBJECTIVE OPTIMIZATION AND DESIGN OF A LUNEBERG LENS ANTENNA WITH MULTIBAND MULTI-POLARIZED FEED-SYSTEM

M. Huang, S. Yang*, J. Teng, Q. Zhu, and Z. Nie

School of Electronic Engineering, University of Electronic Science and Technology of China (UESTC), Chengdu 611731, China

Abstract—A general multiobjective optimization and design procedure of a Luneberg lens antenna (LLA) with a compact multiband multi-polarized feed-system for a broadband satellite communication terminal is presented. The LLA utilizes a compact multiband feed horn, consisting of an inner dielectric loaded circular horn for the K/Ka-band (dual-circular polarization) and a coaxial waveguide with axially corrugated flange for the Ku-band (dual-linear polarization). Measurements show good agreements with simulations. Moreover, an efficient multiobjective evolutionary algorithm based on decomposition (MOEA/D) with differential evolution operator and objective normalization technique is firstly coupled with the vector spherical wave function expansions (VSWE) for the optimal design of a 7-layer 650 mm diameter LLA, which provides higher aperture efficiency at Ku/K/Ka-band simultaneously. The frequency dependence of the LLA is also investigated. Finally, the gain and sidelobe level of a 5-layer design are jointly evaluated and compared with previous works. The proposed design procedure provides much better radiation performances and greater design freedom to the designers, as a group of Pareto-optimal LLA solutions can be obtained with just one simulation.

1. INTRODUCTION

With the growing need for broadband multimedia applications and high speed Internet access, the corresponding electromagnetic spectrum of satellite terminals is being expanded, ranging from 12.2–12.7 GHz (Ku-band downlink), 14–14.5 GHz (Ku-band uplink), 19.7–21.2 GHz (K-band downlink), and 29.5–31.0 GHz (Ka-band uplink). To

Received 10 May 2012, Accepted 13 June 2012, Scheduled 21 June 2012

* Corresponding author: Shiwen Yang (swnyang@uestc.edu.cn).

fully utilize all valuable services, simultaneous multiband and multi-polarized functionality, high aperture efficiency and good port isolation within each operation range are the basic requirements to a satellite terminal. These requirements stimulate an increasing interest in the development of Luneberg lens antennas (LLA) with multiband and multi-polarized feed-system.

LLA system performances strongly depend on the radiation characteristics of the feed system. A good multiband feed horn possesses rotationally symmetric beam width, low cross polarizations and good isolation between transmitting and receiving ports. Various types of feed can be used to illuminate a LLA, such as the multimode horns [1–3], corrugated horns [4–6], dielectric loaded horns [7–10] and coaxial-type horns [11–13]. The bandwidth of the multimode horns is usually limited, but has been improved recently [1]. Dielectric loaded horns have similar antenna performances as compared to corrugated horns but are much simpler and cheaper to fabricate, especially at millimeter-wave band. Coaxial-type horns provide some inherent good isolation between transmitting and receiving bands due to the coaxial geometry, and can also result in a compact structure for easier fabrication [11]. Thus, it is important to choose and design a proper feed satisfying the requirements of the LLA system. Another key challenge in the design of an optimal LLA is to adopt as fewer as possible for the number of lens layers while maintaining higher aperture efficiency at each band and acceptable low sidelobe level (SLL) performance. In the past decades, many analysis methods [14–25] and fabrication techniques [26–33] for lens antennas have been developed. For instance, H. Mosallaei employed genetic algorithm (GA) to control the gain and SLL envelope for a 5-layer 30λ diameter LLA, which offers gain of 37.47 dBi ($\eta_{ap} = 63\%$) with -17.5 dB SLL, yet the optimal solution is largely dependent on the values of the weights specified [16]. Moreover, most of the previous works usually design LLA by using single-objective optimization techniques, such as GA [16], particle swarm optimization (PSO) algorithm [17], differential evolution (DE) algorithm [18, 19], or minmax optimization (MO) algorithm [20], where all the objectives were combined into a single fitness function by adding different weighting factors to different objectives and the selection of the weighting factors depends highly on the rule of thumb. LLAs reported so far are rarely dealt with multiobjective optimization algorithm. T. Maruyama firstly applied Pareto-GA algorithm to balance gain against SLL of the shaped dielectric lens antenna on three principal cut planes [25]. As compared to the conventional single-objective approaches, the main advantage of the multiobjective procedures [34–39] is that multiple conflicting goals

can be jointly evaluated, and many Pareto-optimization solutions can be obtained in a single run without the need of selecting the weighting factors. Thus, the design of a LLA with a compact multiband and multi-polarized feed for a broadband satellite communication terminal, and most of all with well balance in the multi-targets of high gain and low SLL at separated frequency bands become the motivation of this study.

This paper focuses on the multiobjective optimum design of LLAs with multiband multi-polarized feed-system. A compact dual-aperture coaxial-type feed operating at Ku/K/Ka-band with multiple polarizations is presented and experimentally verified. Measurements show good agreements with simulations. In addition, a novel multiobjective evolutionary algorithm based on decomposition (MOEA/D) with differential evolution operator and objective normalization technique is coupled with the vector spherical wave function expansions (VSWE) to fulfill the optimal design of LLA. To our best knowledge, it is the first time that the MOEA/D technique has been applied to the design of LLA. This is especially feasible for the highly efficient design of electrically large size LLA, since the optimum design of entire lens-feed antenna system over the whole frequency range of interest using single-objective optimization techniques becomes unrealistic in each iteration of optimization. It is desired to maximize aperture efficiencies at separated frequency bands simultaneously, while keeping the SLL lower enough to satisfy the specific needs of broadband satellite communication. As compared with methods in previous works [16–20], the proposed design procedure provides much better radiation performances and greater design freedom to the designers, as a group of Pareto-optimal LLA solutions can be readily obtained with just one simulation.

This paper is organized as follows. The design principles and the associated MOEA/D algorithm are described in Section 2, and a novel compact coaxial-type feed of LLA system operating at multiple frequencies and polarizations is designed in Section 3. In Section 4, two numerical examples are discussed to illustrate the potentialities of the proposed methodology. Conclusions are then drawn in Section 5.

2. FUNDAMENTAL LENS ANALYSIS AND MOEA/D

An N-layer LLA of radius R illuminated by a simultaneous Ku/K/Ka-band feed-system is depicted in Figure 1. The variables r_i and ε_i are the outer radius, permittivity of the ith layer, respectively, and f is the feed-to-lens distance. The practical near-field distribution of radiation aperture of the feed at each frequency band is obtained by commercial

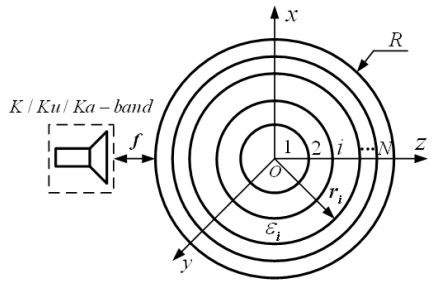

Figure 1. Geometry of an N-layer LLA with a simultaneous Ku/K/Ka-band feed-system.

software CST Microwave Studio, and then separately extracted and discretized into a set of equivalent Huygens sources. When using an infinitesimal electric current element as a feed, the field in ith layer can be formulated as an expansion of the incoming and outgoing travelling spherical wave modes **m** and **n** [15],

$$H_i = \sum_{n=1}^{\infty} \left\{ a_n^i m_{e1n}^{(1)} + b_n^i n_{o1n}^{(1)} + \mathrm{c}_n^i m_{e1n}^{(3)} + d_n^i n_{o1n}^{(3)} \right\} \tag{1}$$

$$E_i = \frac{k_i}{j\omega\varepsilon_i} \sum_{n=1}^{\infty} \left\{ a_n^i n_{e1n}^{(1)} + b_n^i m_{o1n}^{(1)} + \mathrm{c}_n^i n_{e1n}^{(3)} + d_n^i m_{o1n}^{(3)} \right\} \tag{2}$$

where n is the mode number, the superscripts (1) and (3) are the spherical Bessel function of the first kind and Hankel function of the second kind, respectively. The weighting coefficients a_n, b_n, c_n, and d_n are determined by applying the boundary conditions at each interface. The radiation characteristic of a lens-feed antenna system is modeled by using superposition of the fields of the elementary radiators with the appropriate coordinate transformations. Thus, the total field is the integral of Green functions on the radiation aperture of the feed.

Many multiobjective optimization techniques, such as the multiobjective GA [25], multiobjective PSO [34], multiobjective evolutionary algorithm [35–38], and multiobjective differential evolution [39] have recently been successfully applied to electromagnetic problems. In this article, MOEA/D algorithm is adopted for the optimization of LLA with multiband multi-polarized feed-system for a broadband satellite communication terminal. A general definition for a multiobjective optimization problem (MOP) with m objectives can be stated as follows [36]

$$\text{minimize } F(\mathbf{x}) = \{f_i(\mathbf{x}), \quad i = 1, 2, \ldots, m\}, \quad \mathbf{x} \in \Omega \tag{3}$$

where Ω is the decision (variable) space with layer thickness, permittivity, and feed-to-lens distance of the LLA, F: $\Omega \rightarrow R^m$ denotes the objective space with m real-valued objective functions such as aperture efficiency at each band (Ku/K/Ka) and sidelobe level (SLL). Since the objectives in (3) contradict each other very often, no point in Ω minimizes all the objectives simultaneously. One has to balance them and find the best tradeoffs, i.e., Pareto optimality. The set of all the Pareto optimal points $\mathbf{x}^*$ is called the Pareto set (PS) and the corresponding objective vectors $F(\mathbf{x}^*)$ is the Pareto front (PF). To find the Pareto optimal solutions of (3), MOEA/D begins by decomposing the PF into N_{pop} scalar optimization subproblems by using the Tchebycheff approach. The objective function of the jth subproblem is formulated as [36]

$$\text{minimize } g^{te}(\mathbf{x}|\lambda^j, \mathbf{z}^*) = \max_{1\leq i\leq m} \left\{ \lambda_i^j \left| f_i(\mathbf{x}) - z_i^* \right| \right\}, \quad \mathbf{x} \in \Omega \tag{4}$$

$\mathbf{z}^* = \{z_1^*, z_2^*, \ldots, z_m^*\}^T$ is the reference point in the decision space, $\boldsymbol{\lambda}^j = \{\lambda_1^j, \lambda_2^j, \ldots, \lambda_m^j | \sum_{i=1}^m \lambda_i^j = 1\}$ represents the even spread weighting vector. The setting of N_{pop} and $\boldsymbol{\lambda}^j$ is controlled by a parameter H. More precisely, each individual weighting vector λ_i^j takes a value from $\{0, 1/H, 2/H, \ldots, H/H\}$. Therefore, the number of such vectors is $N_{pop} = C_{H+m-1}^{m-1}$. MOEA/D minimizes all these N_{pop} objective functions simultaneously in a single run. A neighborhood of weighting vector $\boldsymbol{\lambda}^j$ is defined based on Euclidean distances between weighting vectors, that is, a set has T ($T < N_{pop}$) closest weighting vectors in $\{\lambda^{j1}, \lambda^{j2}, \ldots, \lambda^{jT}\}$, set $B(j) = \{j_1, j_2, \ldots, j_T\}$. The neighborhood of the jth subproblem consists of all the subproblems with the weighting vectors from the neighborhood of $\boldsymbol{\lambda}^j$. Optimization of each subproblem only uses the current information of its T neighboring subproblems, which makes MOEA/D have lower computational complexity than other techniques such as the nondominated sorting genetic algorithm II (NSGA-II). A simple objective normalization technique [36] is also incorporated into the MOEA/D for dealing with disparately scaled objectives, such as the high gain and low SLL in the LLA design. In this case, the objective f_i ($i = 1, \ldots, m$) in (4) is replaced by $\bar{f}_i = (f_i - z_i^*) / (z_i^{nad} - z_i^*)$, where $\mathbf{z}^{nad} = (z_1^{nad}, \ldots, z_m^{nad})^T$ denotes the nadir point in the objective space, i.e., $z_i^{nad} = \max\{f_i(\mathbf{x})\}$.

The design procedure of LLAs with MOEA/D optimization (Figure 2) has four general steps: initialization, reproduction, update of reference point and neighboring solutions, and update of external population (EP). The reproduction generates the offspring y from its parents $\mathbf{x}^k$ and $\mathbf{x}^l$ by using genetic operators. A polynomial perturbation mutation operator is introduced in reproduction to

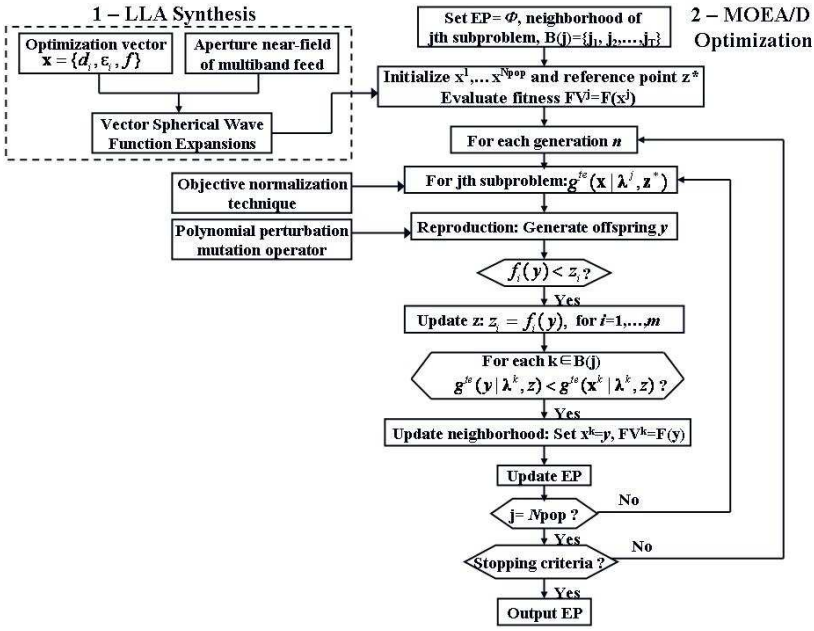

Figure 2. Block diagram of the design methodology of LLAs with MOEA/D optimization.

maintain the population diversity and convergence speed, given by

$$y = \mathbf{x}_i^j + \beta\left(\mathbf{x}_i^k - \mathbf{x}_i^l\right) + \Delta q \cdot (H_i - L_i) \tag{5}$$

$$\Delta q = \begin{cases} \left[2\gamma + (1-2\gamma)\cdot\left(1 - \frac{y - L_i}{H_i - L_i}\right)^{21}\right]^{1/21} - 1, & \gamma \le 0.5 \\ 1 - \left[2(1-\gamma) + 2(\gamma - 0.5)\cdot\left(1 - \frac{H_i - y}{H_i - L_i}\right)^{21}\right]^{1/21}, & \text{otherwise} \end{cases} \tag{6}$$

where $[L_i,\ H_i]$ denotes the search range of the ith optimization parameter for jth subproblem, β is the mutation intensity ($\beta = 0.6$), Δq is the small perturbation, and γ is a real random number in the range $[0, 1]$. Then the reference point z_i is updated, i.e., $z_i = f_i(y)$, if $f_i(y) < z_i$ for each $i = 1, \ldots, m$. Moreover, the neighboring solutions of the jth subproblem are updated: set $\mathbf{x}^k = y$ and evaluate $F(y)$, if $g^{te}(y|\boldsymbol{\lambda}^k, z) \leqq g^{te}(\mathbf{x}^k|\boldsymbol{\lambda}^k, z)$ for each index $k \in B(j)$. Finally, remove all the vectors dominated by $F(y)$ and add $F(y)$ to EP if no vectors in EP can dominate it. In this way, all individuals in the current generation are as good as or better than those in the previous generation. As usual, terminate and output EP if stopping criteria is satisfied.

The proper choice of the parameter T is crucial to the exploration

ability and convergence rate of the MOEA/D algorithm. If T is too small, two solutions chosen ($\mathbf{x}^k$ and $\mathbf{x}^l$) for undergoing genetic operators may be very similar, consequently, the offspring y could be very close to their parents $\mathbf{x}^k$ and $\mathbf{x}^l$. Therefore, the algorithm lacks the ability to explore new areas in the search space. On the other hand, MOEA/D with large T works poorly when the solutions to two subproblems with very different weighting factors are far different, while it performs well when the solutions to two subproblems with very different weighting factors are very similar. Moreover, a too large T will increase the computational load. MOEA/D performs very well with T from 10 to 50 for many applications [36]. The specific parameter value is set by the user for different conditions. In the following description, the neighborhood size T is set to be 10 for all examples.

In this paper, MOEA/D algorithm is applied in the design of LLA with multiband multi-polarized feed-system to meet the stringent requirements of satellite communication. The first example is to maximize aperture efficiency at each frequency band (Ku/K/Ka-band) simultaneously. It is an optimization problem with four objectives ($m = 4$), the objective function of the jth subproblem can be formulated as Equation (7), where η_{0Ka}, η_{0K}, $\eta_{0Kuuplink}$, and $\eta_{0Kudownlink}$ denote the objective aperture efficiency at Ka-band uplink, K-band downlink, Ku-band uplink and Ku-band downlink of satellite communication, respectively.

$$\begin{aligned} &\text{minimize } g_1^{te}\left(\mathbf{x}|\lambda^j, z^*\right) \\ &= \max\left\{\lambda_1^j\left|(1-\eta_{0Ka})-z_1^*\right|, \lambda_2^j\left|(1-\eta_{0K})-z_2^*\right|,\right. \\ &\quad \left.\lambda_3^j\left|(1-\eta_{0Kuuplink})-z_3^*\right|, \lambda_4^j\left|(1-\eta_{0Kudownlink})-z_4^*\right|\right\} \end{aligned} \tag{7}$$

In the second example, the optimization target is to achieve high gain and keep the SLL lower enough to satisfy the specific needs at Ku-downlink band of satellite communication It is an optimization problem with two disparately scaled objectives ($m = 2$), which will further pose challenges to the algorithm. Similarly, this problem can be written as Equation (8), where $dir_{Kudownlink}$ represents the calculated gain of the LLA, g_0 represents the directivity of a uniformly illuminated constant phase aperture. Note that $SLL_{\max}$ is chosen to control the SLL in the angular range $Null_{first} \leq \theta \leq 30^\circ$, where $Null_{first}$ denotes the first null near the main beam.

$$\begin{aligned} &\text{minimize } g_2^{te}\left(\mathbf{x}|\lambda^j, z^*\right) \\ &= \max\left\{\lambda_1^j\left|(1-dir_{Kudownlink}/g_0)-z_1^*\right|, \lambda_2^j\left|SLL_{\max}-z_2^*\right|\right\} \end{aligned} \tag{8}$$

The optimization vector $\mathbf{x}$ is defined by $\mathbf{x} = \{d_i, \varepsilon_i, f, \text{ for } i =$

$1, 2, \ldots, N\}$, where d_i denotes ith layer thickness. The practical near-field aperture distributions of the feed at each frequency band were also taken into account in the multi-frequency optimization. The structural parameters of LLA should satisfy the following equation

$$\begin{cases} d_1 + d_2 + \ldots + d_N = R \\ r_1 = d_1 > d_2, d_3, \ldots, d_N \\ \varepsilon_{i+1} = \varepsilon_i - \Delta\varepsilon_{i+1} \geq 1, \text{ for } i = 1, 2, \ldots N-1 \\ \Delta\varepsilon_{i+1} \geq \sigma_p, \text{ for } i = 1, 2, \ldots N-1 \\ f \in [0, 0.5R] \end{cases} \tag{9}$$

In fact, the thickness of each layer is allowed to change arbitrarily in the range $(0, R)$. However, the larger search range of parameters is time consuming. To achieve a fast optimum design, the innermost layer d_1 should be a little thicker than outer layers. $\Delta\varepsilon_{i+1}$ is the increment permittivity, and σ_p represents the control precision of permittivity for each layer. ε_i is allowed to change between 1.0 to 2.0, and f is selected in $[0, 0.5R]$ to obtain a compromise between spillover efficiency and uniformity of the amplitude distribution of the feed pattern over the LLA.

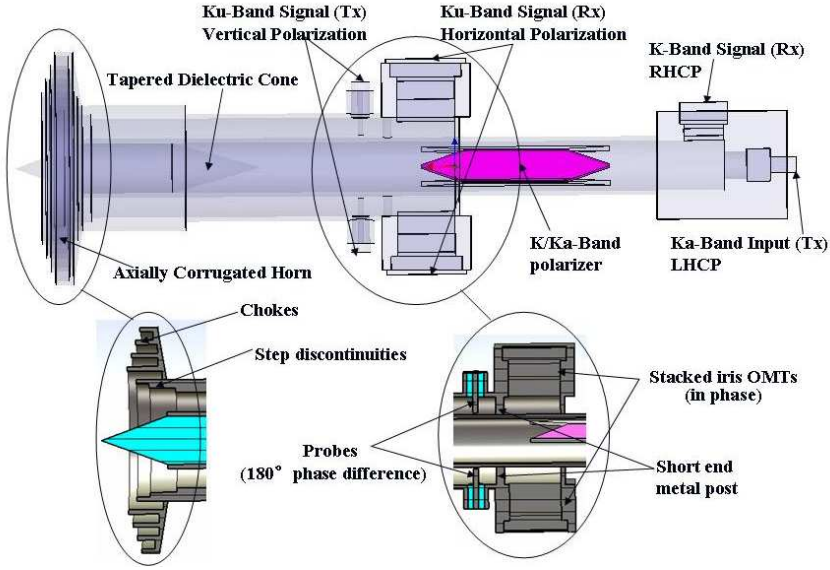

Figure 3. Schematic of a compact coaxial-type feed operating at multiple frequencies (Ku/K/Ka-band) and polarizations.

3. DESIGN OF THE MULTIBAND MULTI-POLARIZED FEED

A compact dual-aperture coaxial feed of LLA system consists of two sections (Figure 3): an inner circular waveguide loaded with a tapered Teflon cone (K/Ka-band, dual-circular polarization) and a coaxial waveguide with axially corrugated flange (Ku-band downlink/uplink, dual-linear polarization), which is capable of tracking the same satellite at uplink and downlink frequencies simultaneously [12]. Radiation characteristics of the tapered Teflon rod ($\varepsilon_r = 2.2$) antenna are dominated by the HE_{11} mode and higher order modes. To avoid exciting higher order modes while operating at K/Ka-band, the diameter of the inner circular waveguide is selected less than 5.7 mm. A good beam equalization and low cross-polar radiation in coaxial feed aperture at Ku-band strongly depend on the outer-to-inner coaxial conductor diameter ratio and the aperture location of the inner horn. Four chokes of different depths placed outside the coaxial waveguide are to suppress the backward radiation and improve the radiation efficiency of the feed. Meanwhile, a number of step discontinuities inside the coaxial waveguide were necessary to improve further the match at Ku band.

To excite the TE_{11} mode and eliminate the undesired but dominate TEM coaxial mode, a pair of probes are fed with 180° phase difference to yield a vertical polarization at Ku-band uplink. The Ku-band downlink horizontal polarization signal is fed through a pair of stacked iris orthomode transducers (OMTs), which exhibit a bandpass characteristic and allow for better impedance matching at Ku-downlink

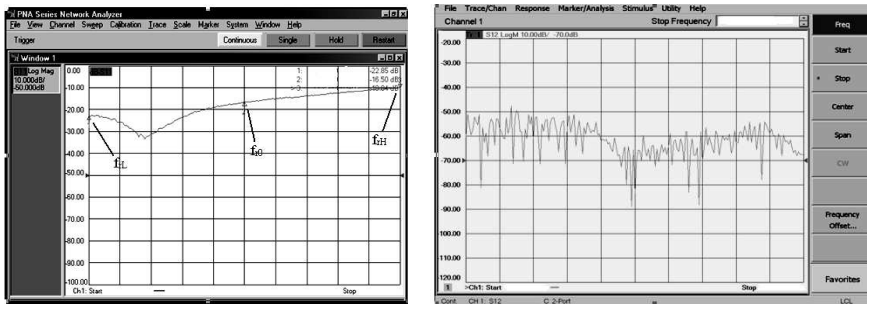

(a) (b)

Figure 4. Measured performances of the Ku-band excitation ports. (a) Return loss of the Ku-band downlink input. (b) Ku-band downlink to uplink port isolation.

band and a high degree of isolation for other bands. Additionally, a short end metal post is applied to reduce the length the coaxial waveguide. Measured performances of excitation ports at Ku-band are shown in Figure 4. The return loss of the Ku-downlink input is better than −10 dB over the desired band. Ku-band downlink to uplink port isolation is very good with a worst case of 50 dB. The K and Ka band signals are fed through OMTs ports at the far end of the inner circular waveguide, respectively. A thin dielectric slab dual-band polarizer [11] is used to transform linear polarization signal into two orthogonal signals with a 90° phase difference to provide dual-circular polarization capability at 20 GHz and 30 GHz. The measured axial ratio is less than 1.86 dB at all frequencies in K-band downlink and Ka-band uplink. The radiation characteristics of the multiband feed are measured in an anechoic chamber. Figure 5 shows the simulated

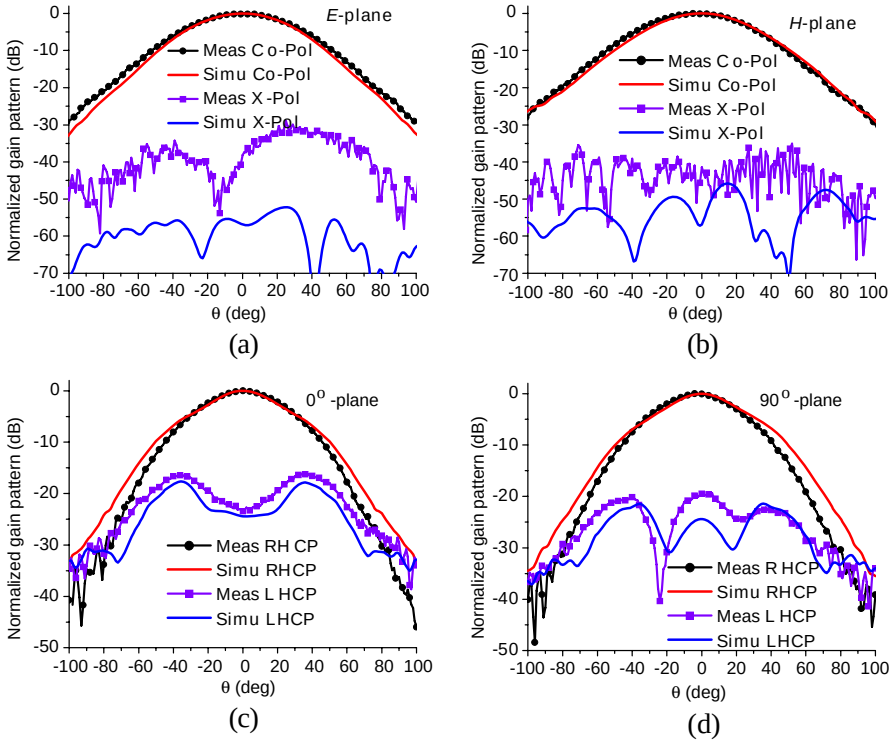

Figure 5. Comparison of the simulated and measured gain patterns of the multiband feed at Ku/K-band, (a) 12.5 GHz at *E*-plane, (b) 12.5 GHz at *H*-plane, (c) 20.5 GHz at 0° cut plane, (d) 20.5 GHz at 90° cut plane.

and measured radiation pattern cuts at Ku/K-band frequencies. The feed possesses rotationally symmetric beams in the principal planes. It has cross-polarization isolation about 30 dB at Ku-band with gain of 10.4 dBi at 12.5 GHz. It also has axial ratio less than 1.86 dB at K/Ka-band with gain of 10.1 dBi at 20.5 GHz. As shown by these figures, the measurement results corroborate the simulation results. Small discrepancies are a result of the manufacturing tolerance.

4. LENS OPTIMIZATION AND DESIGN

In the first example, a 7-layer 650 mm diameter LLA with multiband multi-polarized feed-system (Ku/K/Ka-band) is considered. The optimization goal is to balance the aperture efficiency requirements of LLA at Ku-band downlink/uplink, K-band downlink and Ka-band uplink simultaneously to receive and transmit signals from the same satellite efficiently. It is an optimization problem with four objectives ($m = 4$), $H = 8$, and therefore the size of population is $N_{pop} = 165$. The objective function of the jth subproblem should satisfy Equation (7).

The distributions of 3D Pareto-optimal fronts are shown in Figure 6, where the coordinate values of three axes represent the aperture efficiencies of the optimized LLA at Ku-band downlink/uplink, K-band downlink, and Ka-band uplink. The Pareto fronts found by MOEA/D indicate that aperture efficiencies η_{0ka}, η_{0k} and η_{0ku} are in conflict with each other, since the spillover efficiency and uniformity of the ampli-

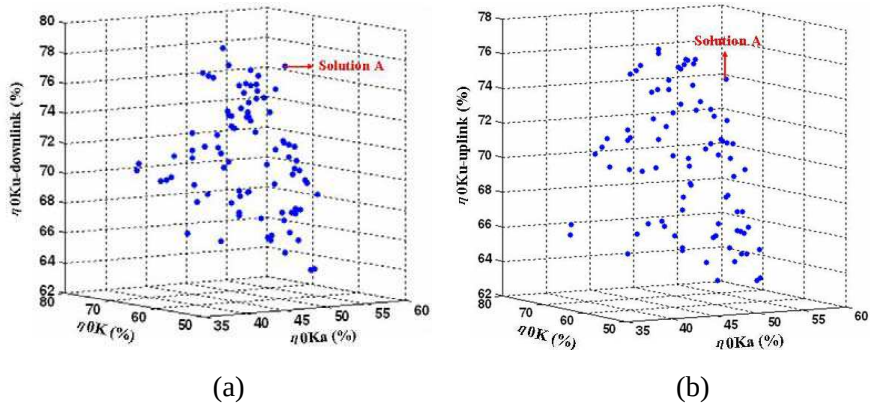

(a) (b)

Figure 6. 3D Pareto fronts for trading off aperture efficiencies at separated frequency bands. (a) Ka-uplink/K-downlink/Ku-downlink. (b) Ka-uplink/K-downlink/Ku-uplink.

tude distribution of the feed pattern over the LLA at these separated bands are slightly different. Pareto fronts provide the antenna designers with optimal alternatives. Each point at the Pareto front represents a Pareto-optimal LLA design, and no absolute perfect solution exists. Solution A shown in Figure 6 is one of the solutions distributed on 3D Pareto-optimal fronts, which has relatively high aperture effi-

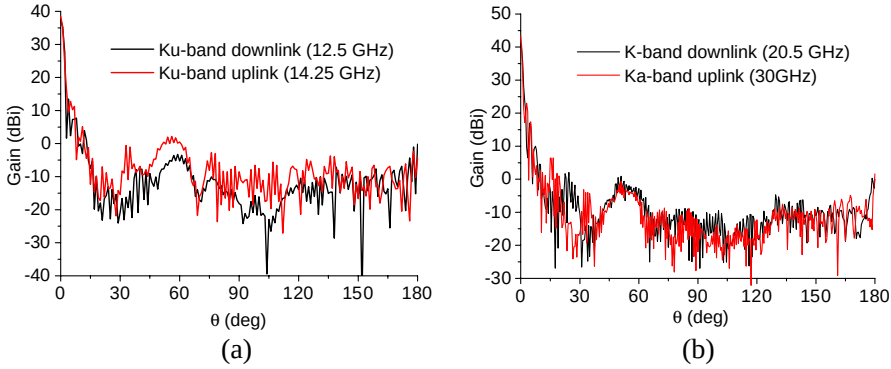

Figure 7. Simulated gain patterns of the 650mm diameter 7-layer LLA (solution A), (a) Ku-band downlink/uplink, (b) K-band downlink and Ka-band uplink.

Table 1. Design parameters of the 7-layer 650 mm diameter LLA (Solution A).

Optimized parameter	Solution A
Layer permittivity ε_i	1.76, 1.70, 1.66, 1.60, 1.53, 1.46, 1.39
Layer thickness d_i (mm)	75, 26, 63, 30, 33, 33,65
Feed-to-lens distance f (mm)	118

Table 2. Radiation characteristics of the 7-layer 650 mm diameter LLA at each band (Solution A).

Frequency	Ku-band downlink	Ku-band uplink	K-band downlink	Ka-band uplink
	12.5 GHz	14.25 GHz	20.5 GHz	30 GHz
Gain (dBi)	37.48	38.48	40.88	43.36
η_{ap} (%)	77.3	74.8	63.2	51.0
Peak SLL (dB)	−24.02	−25.74	−23.85	−20.32

ciency at Ka/K band. For example, if the Ka/K-band performance is more critical than the Ku band performance, solution A is preferred. To illustrate the effectiveness of the algorithm explicitly, simulated gain patterns corresponding to solution A are shown in Figure 7. The simulated gain results of LLA are 37.48 dBi, 38.48 dBi, 40.88 dBi and 43.36 dBi at 12.5 GHz, 14.25 GHz, 20.5 GHz and 30 GHz, respectively, which fulfill the gain requirements of the broadband satellite communication system. The corresponding aperture efficiencies are 77.3%, 74.8%, 63.2% and 51.0%, respectively. The design parameters and radiation characteristics of the 7-layer 650 mm diameter LLA are reported in Table 1 and Table 2, respectively. Moreover, the aperture efficiency and SLL as a function of frequency are shown in Figure 8. It is observed that the LLA maintains nearly stable aperture efficiency at each uplink/downlink band and acceptable low SLL below than −20 dB.

To demonstrate the capability of the design procedure explicitly, the effects of both high gain and low SLL at Ku-band downlink are

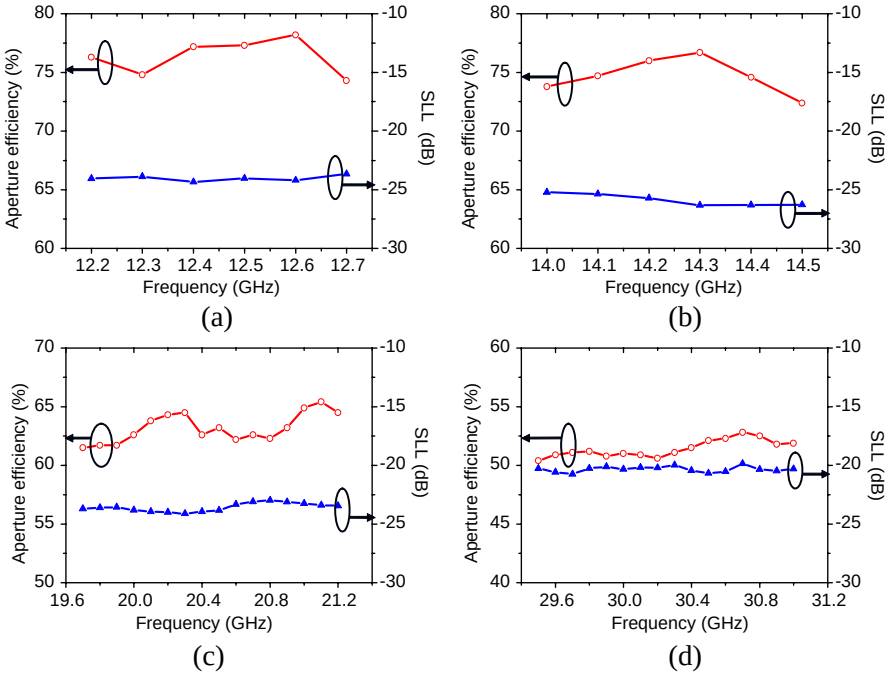

Figure 8. Frequency dependence of the 7-layer optimized LLA. (a) Ku-band downlink. (b) Ku-band uplink. (c) K-band downlink. (d) Ka-band uplink.

jointly evaluated in the process of optimization. It is an optimization problem with two disparately scaled objectives. This problem has been optimized by single-objective optimization approaches, such as GA [16] and PSO algorithm [17]. However, the MOEA/D is applied to optimize the radiation performance of LLA herein to check whether the optimal results reported in [16, 17] can be improved. For fair comparison, an example of a 5-layer 30λ diameter LLA is considered.

The optimization problem has 10 optimization parameters and 100 subproblems. The objective function of the jth subproblem should satisfy Equation (8). Objective normalization approach is introduced into the MOEA/D to deal with the problem. Figure 9 shows the Pareto fronts found by the MOEA/D for trading off the maximum aperture efficiency and peak SLL of the 5-layer 30λ diameter LLA at Ku-band downlink. Specifications of two Pareto-optimal solutions (Solution B and C) are listed in Table 3. As compared with results obtained by GA with different weighting factors ($\alpha = 1$, $\beta = 0$; $\alpha = 1$, $\beta = 0.5$; $\alpha = 0$, $\beta = 1$) [16] and PSO [17], one can find that solution B outperforms the GA/PSO solutions significantly in terms of the peak SLL and maximum gain simultaneously. Solution B offers 38.45 dBi gain ($\eta_{ap} = 78.6\%$) and -25.9 dB SLL at Ku-band

Table 3. Comparison of MOEA/D solutions of the 5-layer 30λ diameter LLA with those optimized by single-objective optimization approaches.

Solutions	MOEA/D		GA [16]			PSO [17]
	B	C	$\alpha = 1$, $\beta = 0$	$\alpha = 1$, $\beta = 0.5$	$\alpha = 0$, $\beta = 1$	
Peak SLL (dB)	-25.9	-28.1	-17.5	-11.9	-15	-
Gain (dBi)	38.45	36.24	37.47	35.94	28	37.2
η_{ap} (%)	78.6	47.4	63	44	7.1	59.1

Table 4. Design parameters and optimal results of the 5-layer 30λ diameter LLA at Ku-band downlink (Solution B).

Parameters	Solution B
Layer permittivity ε_i	1.77, 1.72, 1.66, 1.55, 1.44
Layer thickness d_i (λ)	5.46, 1.33, 2.33,1.96, 3.92
Feed-to-lens distance (λ)	4.33
Gain (dBi)	38.45 ($\eta = 78.6\%$)
SLL (dB)	-25.9

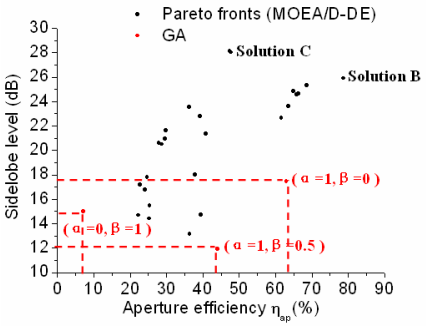

Figure 9. Comparison of optimized solutions obtained from MOEA/D and GA (trading off the maximum aperture efficiency and peak SLL at Ku-band downlink).

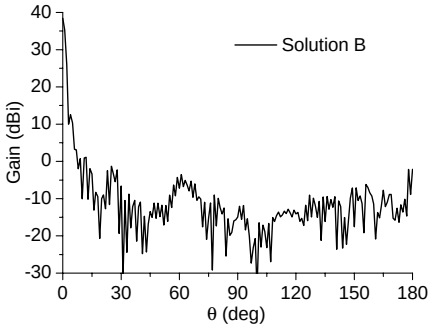

Figure 10. The MOEA/D optimized radiation pattern of the 5-layer 30λ diameter LLA at Ku-band downlink (solution B).

downlink, which helps the increment in aperture efficiency of LLA by 15.6% and the reduction in SLL by 8.4 dB over that obtained by GA [16], and also has a 19.5% improvement in aperture efficiency over that obtained by PSO [17]. Table 4 and Figure 10 show the design parameters and the gain pattern of the 5-layer 30λ diameter LLA at Ku-band downlink (Solution B). On the other hand, although in solution C the gain is dropped by 1.2 dB compared to the previous case ($\alpha = 1$, $\beta = 0$) [16], the SLL is noticeably suppressed under -28.1 dB. The results obtained from MOEA/D demonstrate that many Pareto-optimization solutions can be obtained in a single run without fussy task of selecting weighting factors. The final solution can be chosen from these Pareto-optimization solutions according to the specific design goals.

5. CONCLUSIONS

This paper presents a comprehensive multiobjective optimal design scheme of LLA with multiband multi-polarized feed-system for a broadband satellite communication terminal. A novel compact coaxial-type feed of LLA system operating at Ku/K/Ka-band with multiple polarizations is designed and experimentally verified. The methodology consists in MOEA/D optimization technique based on VSWE that well balances the conflicting specifications of LLA, such as ample aperture efficiency at Ku/K/Ka-band simultaneously, and

high gain and low SLL at Ku-band downlink. The study shows that the proposed method offers great design freedom and various Pareto-optimal LLA solutions to the designers and it is expected to be a particularly attractive optimization tool for other complex electromagnetic problems.

ACKNOWLEDGMENT

This work was supported by National Natural Science Funds for Distinguished Young Scholar under Grant No. 61125104, the National Natural Science Foundation of China under Grant No. 60971030 and the Postgraduate Young Scholarship Award of Ministry of Education of China.

REFERENCES

1. Granet, C., G. L. James, R. Bolton, and G. Moorey, "A smooth-walled spline-profile horn as an alternative to the corrugated horn for wide band millimeter-wave applications," *IEEE Trans. Antennas Propag.*, Vol. 52, No. 3, 848–854, Mar. 2004.
2. Yin, X. H. and S. C. Shi, "A simple design method of multimode horns," *IEEE Trans. Antennas Propag.*, Vol. 53, No. 1, 455–459, Jan. 2005.
3. Agastra, E., G. Bellaveglia, L. Lucci, R. Nesti, G. Pelosi, G. Ruggerini, and S. Selleri, "Genetic algorithm optimization of high-efficiency wide-band multimodal square horns for discrete lenses," *Progress In Electromagnetics Research*, Vol. 83, 335–352, 2008.
4. Carpenter, E., "A dual-band corrugated feed horn," *Proc. IEEE AP-S Int. Symp. Dig.*, Vol. 18, 213–216, Jun. 1980.
5. Kishk, A. A. and C. S. Lim, "Comparative analysis between conical and Gaussian profiled horn antennas," *Progress In Electromagnetics Research*, Vol. 38, 147–166, 2002.
6. Lucci, L., R. Nesti, G. Pelosi, and S. Selleri, "Phase centre optimization in profiled corrugated circular horns with parallel genetic algorithms," *Progress In Electromagnetics Research*, Vol. 16, 127–142, 2004.
7. Clark, P. R. and G. L. James, "Ultra-wideband hybrid-mode feeds," *Electron. Lett.*, Vol. 31, No. 23, 1968–1969, 1995.
8. Chung, J. Y., "Ultra-wideband dielectric-loaded horn antenna with dual-linear polarization capability," *Progress In Electromagnetics Research*, Vol. 102, 397–411, 2010.

9. Xu, O., "Diagonal horn Gaussian efficiency enhancement by dielectric loading for submillimeter wave application at 150 GHz," *Progress In Electromagnetics Research*, Vol. 114, 177–194, 2011.
10. Rolland, A., A. V. Boriskin, C. Person, C. Quendo, L. L. Coq, and R. Sauleau, "Lens-corrected axis-symmetrical shaped horn antenna in metallized foam with improved bandwidth," *IEEE Antennas Wireless Propag. Lett.*, Vol. 11, 57–60, 2012.
11. Stephen, D. T., "A multiband antenna for satellite communications on the move," *IEEE Trans. Antennas Propag.*, Vol. 54, No. 10, 2862–2868, Oct. 2006.
12. Teng, J., S. Yang, and Z. Nie, "Study on multiple frequencies and polarizations feed technique in luneberg lens antenna," *Intelligent Signal Processing and Communication Systems (ISPACS) Int. Symp. Dig.*, Chengdu, Dec. 2010.
13. Bhattacharyya, A., R. Eliassi, C. Hansen, and P. Metzen, "Multiband feed using coaxial configuration," *Int. J. RF Microw. C. E.*, Vol. 21, No. 2, 127–136, 2011.
14. Tai, C. T., "The electromagnetic theory of the spherical luneberg lens," *Appl. Sci. Res.,* Section B, Vol. 7, 113–130, 1958.
15. Sanford, J. R., "Scattering by spherically stratified microwave lens antennas," *IEEE Trans. Antennas Propag.*, Vol. 42, No. 5, 690–698, May 1994.
16. Mosallaei, H. and Y. Rahmat-Samii, "Non-uniform Lüneburg and two-shell lens antennas: Radiation characteristics and design optimization," *IEEE Trans. Antennas Propag.*, Vol. 49, No. 1, 60–69, Jan. 2001.
17. Fuchs, B., R. Golubovic, A. K. Skrivervik, and J. R. Mosig, "Spherical lens antenna designs with particle swarm optimization," *Microw. Opt. Techn. Lett.*, Vol. 52, No. 7, 1655–1659, Jul. 2010.
18. Zhong, M., S. Yang, and Z. Nie, "Optimization of a luneberg lens antenna using the differential evolution algorithm," *Proc. IEEE AP-S Int Symp. Dig.*, San Diego, CA, Jul. 2008.
19. Huang, M., S. Yang, W. Xiong, and Z. Nie, "Design and optimization of spherical lens antennas including practical feed models," *Progress In Electromagnetics Research*, Vol. 120, 355–370, 2011.
20. Fuchs, B., L. Le Coq, O. Lafond, S. Rondineau, and M. Himdi, "Design optimization of multishell Luneberg lenses," *IEEE Trans. Antennas Propag.*, Vol. 55, No. 2, 283–289, Feb. 2007.
21. Fuchs, B., S. Palud, L. Le Coq, O. Lafond, M. Himdi, and

S. Rondineau, "Scattering of spherically and hemispherically stratified lenses fed by any real source," *IEEE Trans. Antennas Propag.*, Vol. 56, No. 2, 450–460, Feb. 2008.

22. Boriskin, A. V., A. Vorobyov, and R. Sauleau, "Two-shell radially symmetric dielectric lenses as low-cost analogs of the Lüneburg lens," *IEEE Trans. Antennas Propag.*, Vol. 59, No. 8, 3089–3093, Aug. 2011.
23. Nikolic, N., J. S. Kot, and S. S. Vinogradov, "Scattering by a Lüneburg lens partially covered by a metallic cap," *Journal of Electromagnetic Waves and Applications*, Vol. 21, No. 4, 549–563, 2007.
24. Vinogradov, S. S., P. D. Smith, J. S. Kot, and N. Nikolic, "Radar cross-section studies of spherical lens reflectors," *Progress In Electromagnetics Research*, Vol. 72, 325–337, 2007.
25. Maruyama, T., K. Yamamori, and Y. Kuwahara, "Design of multibeam dielectric lens antennas by multiobjective optimization," *IEEE Trans. Antennas Propag.*, Vol. 57, No. 1, 57–63, 2009.
26. Carpenter, M. P., et al., "Lens of gradient dielectric constant and methods of production," US Patent 6433936 B1, 2001.
27. Rondineau, S., M. Himdi, and J. Sorieux, "A sliced spherical Lüneburg lens," *IEEE Antennas Wireless Propag. Lett.*, Vol. 2, 163–166, 2003.
28. Wang, G., Y. Gong, and H. Wang, "On the size of left-handed material lens for near-field target detection by focus scanning," *Progress In Electromagnetics Research*, Vol. 87, 345–361, 2008.
29. Andrés-García, B. and L. E. García-Muñoz, "Filtering lens structure based on SRRs in the low THz band," *Progress In Electromagnetics Research*, Vol. 93, 71–90, 2009.
30. Ma, H. F., X. Chen, H. S. Xu, X. M. Yang, W. X. Jiang, and T.-J. Cui, "Experiments on high-performance beam-scanning antennas made of gradient-index metamaterials," *Appl. Phys. Lett.*, Vol. 95, 094107, 2009.
31. Ma, H. F., X. Chen, X. M. Yang, W. X. Jiang, and T.-J. Cui, "Design of multibeam scanning antennas with high gains and low sidelobes using gradient-index metamaterials," *J. Appl. Phys.*, Vol. 107, 014902, 2010.
32. Dou, W. B., Z. L. Sun, and X. Q. Tan, "Fields in the focal space of symmetrical hyperbolic focusing lens," *Progress In Electromagnetics Research*, Vol. 20, 213–226, 1998.
33. Zhang, Z. and W. Dou, "Binary diffractive small lens array for Thz imaging system," *Journal of Electromagnetic Waves and*

Applications, Vol. 25, Nos. 2–3, 177–187, 2011.

34. Chamaani, S., S. A. Mirtaheri, M. Teshnehlab, M. A. Shooredeli, and V. Seydi, "Modified multi-objective particle swarm optimization for electromagnetic absorber design," *Progress In Electromagnetics Research*, Vol. 79, 353–366, 2008.
35. Lee, Y. H., B. J. Cahill, S. J. Porter, and A. C. Marvin, "A novel evolutionary learning technique for multi-objective array antenna optimization," *Progress In Electromagnetics Research*, Vol. 48, 125–144, 2004.
36. Zhang, Q. and H. Li, "MOEA/D: A multiobjective evolutionary algorithm based on decomposition," *IEEE Trans. Evol. Comput.*, Vol. 11, No. 6, 712–731, Dec. 2007.
37. Pal, S., S. Das, and A. Basak, "Design of time-modulated linear arrays with a multi-objective optimization approach," *Progress In Electromagnetics Research B*, Vol. 23, 83–107, 2010.
38. Chen, Y., S. Yang, and Z. Nie, "Improving conflicting specifications of time-modulated antenna arrays by using a multiobjective evolutionary algorithm," *Int. J. Numer. Model. El.*, Jul. 2011.
39. Goudos, S. K., K. Siakavara, E. E. Vafiadis, and J. N. Sahalos, "Pareto optimal Yagi-Uda antenna design using multi-objective differential evolution," *Progress In Electromagnetics Research*, Vol. 105, 231–251, 2010.